International Journal of Innovative
Computing, Information and Control
Volume **12**, Number **5**, October **2016**

ICIC International ©2016 ISSN 1349-4198
pp. 1597–1613

SYNCHRONIZATION ANALYSIS OF THE PRODUCTION PROCESS UTILIZING THE PHASE-FIELD MODEL

Kenji Shirai[1] and Yoshinori Amano[2]

[1]Faculty of Information Culture
Niigata University of International and Information Studies
3-1-1, Mizukino, Nishi-ku, Niigata 950-2292, Japan
shirai@nuis.ac.jp

[2]Kyohnan Elecs Co., LTD.
8-48-2, Fukakusanishiura-cho, Fushimi-ku, Kyoto 612-0029, Japan
y_amano@kyohnan-elecs.co.jp

Received February 2016; revised June 2016

Abstract. *We analyze the cause of fluctuations in the lead time of production processes by applying a phase-field model, which is a new approach. Occurrence factors are attributed to state variables in an internal process. The factors of such fluctuations are an uncertainty of logistics, uncertainty of production planning, and stochastic characteristics of the order and start time series. These fluctuations are found to affect production costs. We represent a mathematical model to constrain the throughput deviation; this model is dependent on volatilities that are generated from both inside and outside noise.*
Keywords: Phase-field, Throughput deviation, Lead time, Potential, Production process

1. **Introduction.** Many currently implemented production systems are mechanized and highly integrated with information technologies, which creates systems where human intervention is unnecessary. In certain aspects of the production system, there is a high volume of build-to-order manufacturing that requires human intervention in the production process [1, 2]. In small- and medium-sized enterprises, human intervention constitutes a significant part of the production process, and revenue can sometimes be greatly affected by human behavior. Therefore, with respect to human intervention with outside companies, a deep analysis of the production process and human collaboration is necessary to understand the potential negative effects of human intervention [1, 2]. Naturally, the effect of human behavior is not just a problem with small- and medium-sized companies; it must be regarded as one of the major problems that may occur when humans directly intervene in the production process [3, 4, 8].

In general, the potential uncertainties should be considered before proceeding with a system that combines human intervention (Internal force) with outside companies (External force) in the production system [5, 6]. With respect to two elements in a production system, a total system is formed by connecting the two elements. In this case, a system with certain uncertainties will be formed when connecting "human intervention" and "outside companies" in a production system. In general, an important concept in the production system is to develop the best system that results in efficient production. However, in most analysis of the production process, researchers have not taken advantage of the noise inherent in the system. Such noise may have a unique usefulness in the system.

Thus, we have been researching mathematical modeling and system evaluations from a physical point of view to develop "mathematical production engineering", in order to

develop a mathematical system for describing production processes. In a previous study of stochastic modeling, we considered the internal force and external force as parameters in a production system. The correlation of lead time vs. throughput is important for implementing the overall synchronization as a strategy. We had reported a production system with an intervention of workers in the prior study [5, 6]. In case of a production flow system with human intervention, we need to fulfill an empirical analysis of worker-specific production ability. Thus, to achieve optimal general production systems, knowledge of the importance of biological fluctuations in the system is important.

In our previous study, an on-off intermittency exists in the rate-of-return and lead time deviations of production processes. In physics, an on-off intermittency is present in case of power-law distributions, phase transitions, and self-similar phenomena. In the production process described in this study, we observed on-off intermittency on lead time data with respect to time series outset [7].

Previously, we have reported that by creating a state in which the production density of each process corresponds to physical propagation, the manufacturing process is most appropriately described using a diffusion equation [1]. In other words, if the potential of the production field (stochastic field) is minimized, the equation is defined by the production density function $S_i(x,t)$ and the constraint is described using an advective diffusion equation to determine the transportation speed ρ [1, 20].

To enable efficient application to a production system, we have proposed a mathematical model that focuses on the selection process and production lead time adaptation mechanism. To model the throughput time for a production demand/manufacturing system in the manufacturing stage, the dynamic behavior is derived using a lognormal stochastic differential equation. Using this model, the evaluation equation for the compatibility condition production lead time is defined using the risk-neutral integral, and the evaluation formula for the above conditions is calculated. Furthermore, by performing the synchronization process, the throughput for the manufacturing process is reduced [2].

We have been studying throughput improvements and factors in production processes from the viewpoint of physical and mathematical properties. In this study, we represented the analysis of the throughput (lead time) fluctuation in a production system by applying a phase-field model. The factors of this fluctuation are as follows.

- Uncertainty of logistics
- Uncertainty of production planning
- Stochastic characteristics of the order and start time series

In this study, we report on production throughput improvement method by combining the diffusion equation with the phase-field method. The phase-field method is a continuous model in inhomogeneous field with an order parameter. The fluctuation of lead time in the process is caused by restraining the Burgers equation in the fluid dynamics; that is, the propagation of state variables, which denotes a throughput deviation between processes in this case, shows the fluctuation. At this time, the start time series of period lead time in the production processes have an on-off intermittent characteristics.

We present the actual data, derived from the fluctuation of the throughput average data, for the starting time series (order time-series) of production from customers. We also represent a potential function in the phase-field model for the throughput volatility as the main parameter.

Our theoretical study can be applied for throughput analysis. Volatility reduction in production processes is very important. The production efficiency of a synchronization process for a flow production system became clear from the actual data. For further

verification, we confirmed the benefit of using this process for the system by performing a dynamic simulation. To the best of our knowledge, this is the first study on the contribution of fluctuations to production processes.

2. Description of Ginzburg-Landau (G-L) Free Energy.

2.1. **Cyclic production flow process.** Figure 1 depicts a production process that is termed as a production flow process. This production process is employed in the production of control equipment. In this example, the production flow process consists of six stages. In each step S1-S6 of the production process, materials are being produced.

The direction of the arrows represents the direction of the production flow. In this process, production materials are supplied through the inlet and the end-product is shipped from the outlet. For this flow production system, we make the following two assumptions.

2.2. **Description of potential energy.** The purpose of this subsection is to guide the gradient system from potential energy and Ginzburg-Landau (G-L) free energy equation [9]. In our previous study, we reported the multimode vibration analysis in terms of the average potential energy [10]. Kuramitsu and Nishikawa certified that the structure is derived using the van der Pol equation [11, 12]. Moreover, data gathered from a production flow process indicates that all production stages correlate with each other. Thus, according to the method proposed by Kuramitsu and Takase, Figure 1 indicates a production flow process using the circuit diagram shown in Figure 2 [11, 12]. In Figure 2, "osc" indicates the working-time delay at each stage in the process.

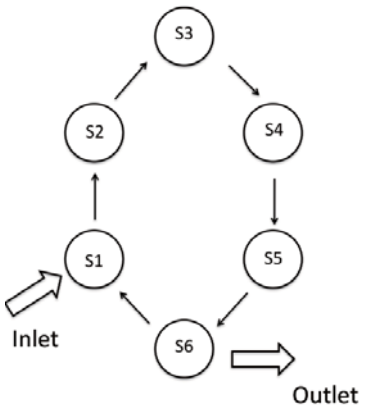

FIGURE 1. Cyclic production flow process

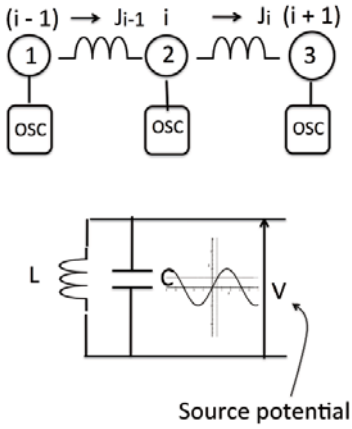

FIGURE 2. Lattice model for electric circuit

From discrete model [13], we define the flow of Figure 2.

Definition 2.1. *Discrete stage model shown as Figure 2*

$$J_i(\alpha, t) = \max\left(0, \min\left(L_i(t), \tilde{J}_i(\alpha, t)\right)\right) \tag{1}$$
$$\tilde{J}_i(\alpha, t) = \alpha r_i(t - d_i) - D_i\left(n_{i+1}(t - d_i) - n_i(t)\right)$$

where $L_i(t)$ is the constraint function between processes, d_i is the time delay, α is a constant and n_i is the working time at process i.

Then, let a delay elements be as follows:

$$D = \frac{D_i}{d_i}$$

where D is an overall diffusion coefficient.

$$\tilde{J}_i(\alpha, t, x) = \alpha n(x,t) - D\frac{\partial n(x,t)}{\partial x} \tag{2}$$

$$\frac{\partial n(x,t)}{\partial t} = -\alpha\frac{\partial n(x,t)}{\partial x} + D\frac{\partial^2 n(x,t)}{\partial x^2}, \quad \frac{\partial n(x,t)}{\partial t} = -\frac{\partial \tilde{J}(\alpha,t,x)}{\partial x} \tag{3}$$

From Equation (75) in Appendix B, we similarly defined the overall stage average $h_I(t)$ as follows.

Definition 2.2. *Overall stage average* $h_I(t)$

$$h_I(t) = \frac{\sum_i S(i,t)}{[\Omega]} \tag{4}$$

h_0 at equilibrium is as follows:

$$h_0(t) \equiv \frac{\sum_i S(t)}{[\Omega]} \tag{5}$$

Then, we obtain as follows:

$$h_I(t+\Delta t) - h_I(t) = -\frac{h_I(t) - h_0}{D} + \bar{O}(\epsilon)\Delta t \tag{6}$$

$S(i,t)$ is a process load at i process and Ω_i is the i-th process.

We ignored the second-order term of Equation (6) and converted the variable $h_i(t)$.

$$\frac{\partial h^{(1)}(t)}{\partial t} = -\frac{h^{(1)}(t) - h_0}{D} \tag{7}$$

where $h_I(t)$ is expanded as follows:

$$h_I(t) = h^{(1)}(t) + \epsilon u(t) + O(\epsilon^2) \tag{8}$$

Definition 2.3. *$P_I(x < h_I(t) < x + dx)$ is a probability density function, where x is a positive real number.*

From statistical mechanics, we obtain as follows:

$$\frac{\partial}{\partial t}P_I(x,t) = \sum_{n=1}^{\infty}\frac{(-1)^n}{n!}\epsilon^{n-1}\left(\frac{\partial}{\partial x}\right)^n C_n(x,t)P_I(x,t) \tag{9}$$

$$C_n(x,t) = \int r^n w(t,x,r)dr$$

where $C_n(x,t)$ is the n-th moment of $w(t,x,r)$. $w(t,x,r)$ is a transition rate from $h_I = x$ to $x + r$. Equation (9) is called Kramers-Moyal expansion [14, 15].

Definition 2.4. *Characteristic function $Q(t,\xi)$ of $P_I(x,t)$*

$$Q(t,\xi) = \int P_I(x,t)e^{i\xi x}dx \tag{10}$$

Definition 2.5. *Characteristic function $w(t,\xi)$ of the transition rate*

$$w(t,r,\xi) = \int w(t,r,x)e^{i\xi x}dx \tag{11}$$

The master equation of $Q(t,\xi)$ is as follows:

$$\frac{\partial}{\partial t}Q(t,\xi)=\frac{1}{2\pi}\int dr\int d\eta\int_0^r dsi\xi e^{i\epsilon\xi s}Q(t,\xi-\eta)w(t,r,\eta) \tag{12}$$

where the solution of $Q(t,\xi)$ is as follows:

$$Q(t,\xi)=\exp(g(x,t))=\exp\left[\sum_{n=1}^{\infty}\frac{(i\xi)^n}{n!}g_n(t)\right] \tag{13}$$

where $g_n(t)$ is the n-th cumulant of h_I [19].

According to Equation (8), $g_n(t)$ is as follows:

$$g_1(t)=y(t)+\epsilon u(t)+\bar{O}(\epsilon^2) \tag{14}$$

$$g_2(t)=\epsilon v(t)+\bar{O}(\epsilon^2) \tag{15}$$

We obtain as follows:

$$\frac{\partial y(t)}{\partial t}=C_1(t,y) \tag{16}$$

$$\frac{\partial v(t)}{\partial t}=2C_1^{'}(t,y)v(t)+C_2(t,y) \tag{17}$$

$$\frac{\partial u(t)}{\partial t}=C_1^{'}(t,y)u(t)+\frac{1}{2}C_1^{''}(t,y)u(t) \tag{18}$$

where $C_1^{'}$ and $C_1^{''}$ denote the first and second derivatives of C_1 with respect to y respectively. Note that the temporal evolution of the cumulants is determined by the moments of the transition rate.

According to Equation (7), Equation (16) is as follows:

$$C_1(t,y)=-\frac{y-y_0}{D} \tag{19}$$

Further, we assume as follows.

Assumption 2.1. *$C_2(t,y)$ denotes a constant data* [13, 19].

$$C_2(t,y)=b_r=const. \tag{20}$$

where $C_2(t,y)$ denotes a constant like Brownian motion.

We obtain as follows:

$$\frac{\partial y(t)}{\partial t}=C_1(t,y)=-\frac{y-y_0}{D} \tag{21}$$

$$\frac{\partial v(t)}{\partial t}=2\left(-\frac{1}{D}\right)v(t)+b_r \tag{22}$$

$$\frac{\partial u(t)}{\partial t}=-\frac{1}{D}u(t) \tag{23}$$

Then, $P_I(x,t)$ is the solution of Fokker-Planck equation.

$$\frac{\partial}{\partial t}P_I(x,t)=-\left[-\frac{\partial}{\partial x}C_1(x,t)+\epsilon\frac{1}{2}\frac{\partial^2}{\partial x^2}C_2(x,t)\right]P_I(x,t) \tag{24}$$

Let $v(t)$ be as follows:

$$v(t)=\frac{b_rD}{2}\left(1-e^{-2t/D}\right) \tag{25}$$

Then,

$$\lim_{t\to\infty} v(t) = \frac{b_r D}{2} \tag{26}$$

Let the initial value of $P_I(x,t)$ be as follows:

$$P_I(x,t) = \delta(x - x_0) \tag{27}$$

From Equation (24), non-equilibrium distribution of $P_I(x,t)$ near equilibrium state is as follows:

$$P_I(x,t) = \frac{1}{\sqrt{2\pi\epsilon v(t)}} \exp\left[-\frac{\left\{ x - y_0 - (x_0 - y_0)e^{-\frac{t}{D}} \right\}^2}{2\epsilon v(t)} \right] \tag{28}$$

Then from Equation (28), let $t \to \infty$,

$$\lim_{t\to\infty} P_I(x,t) = \frac{1}{\sqrt{\pi\epsilon b_r D}} \exp\left[-\frac{(x - y_0)^2}{\epsilon b_r D} \right] \tag{29}$$

where $C_1(x,t)$ and $C_2(x,t)$ denote the drift coefficient and diffusion coefficient respectively.

Moreover, we assume as follows.

Assumption 2.2.

$$P_I(x,t) = 0, \quad P_I(x,t) = +P_L, \quad P_I(x,t) = -P_L \tag{30}$$

where $P_I(x,t) = 0$ denotes stable point (Synchronous state), and $P_I(x,t) = +P_L$ and $P_I(x,t) = -P_L$ denote both of asynchronous transition state.

Further the mathematical model of $h_I(t)$ is derived by Langevin equation [16].

$$\frac{dh_I(t)}{dt} = F(t, h_I) + \sqrt{H} r(t) \tag{31}$$

According to Vasicek model [6],

$$\frac{dh_I(t)}{dt} = a\left\{ W_{opt}\left(\Delta\varphi\right) - h_I(t) \right\} + \sqrt{H} r(t) \tag{32}$$

where $\Delta\varphi = h_I(t) - h_I^0$. h_I^0 denotes an equilibrium point (synchronous point) and $W_{opt}(\Delta\varphi)$ denotes an optimal throughput function, which was calculated according to $\Delta\varphi$, and is a C^∞ function.

From Equation (31) and Equation (32), we can consider as follows:

$$F(t, h_I) = a\left\{ W_{opt}(\Delta\varphi) - h_I(t) \right\} \tag{33}$$

where the throughput deviation $\Delta\varphi = h_I(t) - h_I^0$.

Then let the transition probability density function be $W_I(t, h_I)$,

$$\frac{\partial W_I}{\partial t} = -\frac{\partial}{\partial h_I} F(t, h_I) W_I(t, h_I) + H \frac{\partial^2 W_I}{\partial h_I^2} \tag{34}$$

$W_I(t, h_I)$ is derived by Fokker-Plank equation.

$$\frac{\partial P_I}{\partial t} = -C_1(t, h_I)\frac{\partial P_I}{\partial h_I} + C_2(t, h_I)\frac{\partial^2 P_I}{\partial h_I^2} \tag{35}$$

Let $F(t, h_I) \equiv a\left\{ W_{opt}(\Delta\varphi) - h_I(t) \right\}$,

$$\frac{\partial W_I}{\partial t} = -\frac{\partial}{\partial h_I}\left[a\left\{ W_{opt}(\Delta\varphi) - h_I(t) \right\} \right] W_I(t, h_I) + H \frac{\partial^2 W_I}{\partial h_I^2} \tag{36}$$

From nonlinear scaling theory [15], we obtain the following Fokker-Plank equation [13, 19].

Lemma 2.1.

$$\frac{\partial P_I}{\partial t} = \left[\frac{\partial}{\partial h_I}\left(-rh_I + gh_I^3\right) + \frac{b_r}{2}\frac{\partial^2}{\partial h_I^2}\right] P_I \tag{37}$$

We simplify as follows:

$$\frac{dh_I}{dt} = \alpha\left(h_I(t)\right) + \beta\left(h_I(t)\right) Z(t) \tag{38}$$

where $< Z(t) \cdot Z(t^{'}) >= 2\epsilon\delta(t - t^{'})$.

$\alpha\left(h_I(t)\right)$ is derived as follows:

$$\alpha(h_I(t)) \approx rh_I(t) + (\text{Higher-order term}) \tag{39}$$

where $\alpha(h_I(t))$ can be deployed in the vicinity of $h_I(t) = 0$ and $r > 0$.

Then the scaling vairiable $\tau(t)$ is as follows:

$$\tau(t) \equiv \epsilon w(t), \quad \tau \equiv \epsilon \exp(2rt) \tag{40}$$

The fluctuation $< |h_I(t)|^2 >$ is as follows:

$$< |h_I(t)|^2 >=< h_I^2 >_{st} \cdot f^{(sc)}(\tau) \tag{41}$$

Then, we introduce as time dependent Ginzburg-Landau (TDGL) equation,

$$\frac{\partial P_I(x,t)}{\partial t} = \left\{r - g\varphi^2(x,t)\right\}\varphi(x,t) + D\bigtriangledown^2\varphi(x,t) + \eta(x,t) \tag{42}$$

where $< \eta(x,t) \cdot \eta\left(t^{'}, x^{'}\right) >= 2\epsilon\delta\left(t - t^{'}\right)$ and let the initial condition be $\varphi(0,x) = \varphi_0\delta\left(\frac{x}{r_0}\right)$.

Thus, $\varphi(x,t)$ denotes an order parameter, such as the throughput (lead time) deviation between processes. Generally, the potential energy of a system is set to $f(\varphi)$.

Definition 2.6. *G-L free energy*

$$F(\varphi) = \int_\Omega \left[\frac{\epsilon^2}{2}|\bigtriangledown\varphi|^2 + f(\varphi)\right] dV \tag{43}$$

According to our previous study [16], we define as follows.

Definition 2.7. *Gradient system*

$$\frac{\partial\varphi}{\partial t} = -\frac{\delta F(\varphi)}{\delta\varphi} \tag{44}$$

where $\frac{\delta F(\varphi)}{\delta\varphi}$ *denotes a functional derivative* [15].

G-L free energy is written with respect to Equation (44) as follows:

$$\frac{\partial\varphi}{\partial t} = -\frac{\delta F(\varphi)}{\delta\varphi} = \epsilon^2\bigtriangledown^2\varphi - f'(\varphi) \tag{45}$$

2.3. **Description of the phase-field model.** We define a phase-field model as follows.

Definition 2.8. *Phase-field model*

$$f(\varphi) = ag(\varphi) + bh(\varphi) + c(1 - h(\varphi)) \tag{46}$$

where b and c denote liquid and solid phases, respectively. These parameters are dependent on the dispersion of non-occurrence probability that depends on the noise intensity in production processes.

Figure 3 denotes a double well potential function, which is $\varphi^2(1-\varphi)^2$.

Then according to a phase-field model [17], the particular solution of $h(\varphi)$ like $\varphi^2(1-\varphi)^2$ is denoted as follows:

$$\varphi(x,t) = \frac{1}{2}\left[1 - \tanh\left\{\frac{a(x-V)}{2\epsilon}\right\}\right], \quad V = \frac{6\epsilon(c-b)}{a\tau} \tag{47}$$

The direction of a particular solution has been suggested a transition from $\varphi(x,t) = 1$ to $\varphi(x,t) = 0$ with respect to x in Equation (45).

Next, we denoted the static solution at $V - 0$, where we assumed that the condition was $b = c$. Considering $t = 0$ in Equation (47), we obtained as follows:

$$\varphi_0(x) = \frac{1}{2}\left[1 - \tanh\left\{\frac{ax}{2\epsilon}\right\}\right] \tag{48}$$

From Equation (45), it is written as follows:

$$\epsilon^2 \frac{d^2\varphi_0(x)}{dx^2} - f'(\varphi_0) = 0 \tag{49}$$

When we run the integration to Equation (49) after multipling $\left(\frac{d\varphi_0}{dx}\right)$ on both sides of that, then it is written as follows:

$$\int_\Omega \epsilon^2 \left[\frac{d^2\varphi_0(x)}{dx^2}\right]\left(\frac{\varphi_0}{dx}\right)dx - \int_\Omega \frac{\partial f(\varphi_0)}{\partial \varphi_0}\left(\frac{d\varphi_0}{dx}\right)dx = 0 \tag{50}$$

From Equation (50), we obtain as follows:

$$\epsilon^2\left[\frac{\varphi_0}{dx}\right]^2 - f(\varphi_0) = C \tag{51}$$

where C is an integration constant.

With respect to Equation (51), as $|x| \to \infty$, $C = 0$.

Therefore, it is written as follows:

$$\epsilon^2\left[\frac{\varphi_0}{dx}\right]^2 = f(\varphi_0) \tag{52}$$

Moreover, it is written as follows:

$$\frac{\varphi_0}{dx} = \frac{\sqrt{2f(\varphi_0)}}{\epsilon} \tag{53}$$

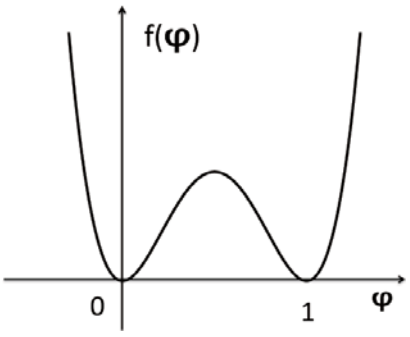

FIGURE 3. Double well potential

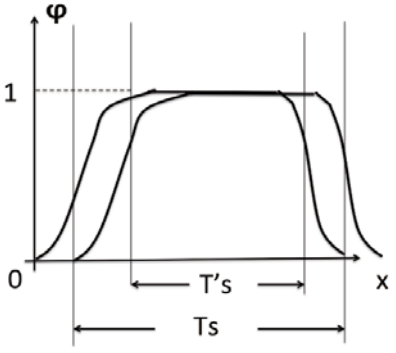

FIGURE 4. Transition width of lead time

From Equation (53), G-L energy is written as follows:

$$F(\varphi_0) = \int_{-infty}^{\infty} \left[\frac{\epsilon^2}{2} \left(\frac{d\varphi_0}{dx} \right)^2 + f(\varphi_0) \right] dx = \int_{-infty}^{\infty} 2f(\varphi_0) dx = \int_0^1 2f(\varphi_0) \frac{dx}{d\varphi_0} \cdot d\varphi_0$$
$$= \int_0^1 2f(\varphi_0) \left(\frac{d\varphi_0}{dx} \right)^{-1} d\varphi_0 = \epsilon \int_0^1 \sqrt{2f(\varphi_0)} d\varphi_0 \tag{54}$$

Therefore, if $f(\varphi_0)$ is determined, a transition boundary width (phase transition width) $F(\varphi_0)$ can be obtained (See Figure 4).

From Figure 4, the transition area ΔT_s is written as follows:

$$\Delta T_s = T_s - T_s^{'} \tag{55}$$

where ΔT_s denotes the lead time transition.

ΔT_s is influenced by the noise intensity or it is depending on volatility of non-normal probability.

3. **Relation between Fluctuations and Potential Energy.** In Figure 5, it is to modulate only the phase difference θ for the fundamental period T_0 was observed to modulate. Main causes were dependent on an endogenous disturbance and stochastic worker abilities, which are outside forces of basic potential energy in production processes. Figure 6 shows the potential energy in terms of the time variable in the phase.

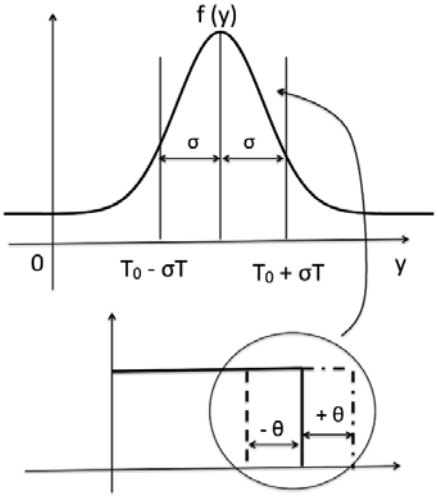

FIGURE 5. Probability distribution of fluctuations and throughput threshold

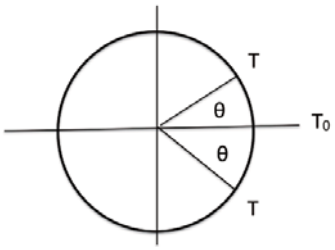

FIGURE 6. Concept of phase for lead time potential energy

The potential energy is written as follows:

$$V(\theta) = \sigma \cdot \theta + B(-4C \cos\theta + \cos 2\theta) \tag{56}$$

where σ denotes a volatility of endogenous disturbance. Specifically, σ denotes the volatility of stochastic throughput $C(t)$ [18]. Then, $\sigma \approx K_\sigma$ and K_σ denotes a real number.

Therefore, Equation (56) is deformed as

$$V(\theta) = K_\sigma \cdot \theta + B(-4C \cos\theta + \cos 2\theta) \tag{57}$$

According to Table 1, $K_\sigma \approx 0.29$ in test run1, $K_\sigma \approx 0.06$ in test run2, and $K_\sigma \approx 0.03$ in test run3 (see Table 1).

TABLE 1. Correspondence between the table labels and the test-run number

	Production process	Working time	Volatility
test run1	Asynchronous process	627(min)	0.29
test run2	Synchronous process	500(min)	0.06
test run3	"Synchronization with preprocess" method	470(min)	0.03

According to the value of K_σ, the potential energy was displaced and changed the direction of the deviation of the displaced by the positive and negative of the value of K_σ. According to test run1 through test run3 of our production flow system obtained using the actual data, the coefficient for the external force denoted a parameter that indicated the ability to execute against the lead time of workers. In other words, the use of the volatility led to the same results as the use of the uncertainty factor. Please refer to our previous study for the actual data [4, 6].

The production throughputs are as follows. Here, the trend coefficient, which is the actual number of pieces of equipment/the target number of equipment, represents a factor that indicates the degree of the number of pieces of manufacturing equipment.
test run1: 4.4 (pieces of equipment)/6 (pieces of equipment) = 0.73,
test run2: 5.5 (pieces of equipment)/6 (pieces of equipment) = 0.92,
test run3: 5.7 (pieces of equipment)/6 (pieces of equipment) = 0.95.

4. **Consideration of the Practical Meaning of the Parameters B and C.** If we can define parameters B and C, we can explicitly denote the potential function for the deviation (phase) of a set value. A useful technique is to combine a threshold of the determination of the lead time using stochastic resonance (throughput) so that we can obtain in forming a mathematical model of production processes.

The potential energy may change a certain direction according to an external force. The transition of the lead time threshold value mainly depends on the volatility of production processes. Therefore, by setting the volatility of a synchronization process to σ_s and that of a real process to σ, we defined the potential energy function using a phase-field method as follows.

Definition 4.1. *Potential energy function* $f(\varphi)$

$$f(\varphi) = ag(\varphi) + b_S h(\varphi) + C_L\{1 - h(\varphi)\} \tag{58}$$

From the relationship between σ_s and σ, we classify as follows.

[1] as $\sigma_s = \sigma$, $\quad 0 = b_S = C_L \quad T_s = T$
[2] as $\sigma_s < \sigma$, $\quad 0 = C_L < b_S \quad T_s < T$
[3] as $\sigma_s > \sigma$, $\quad 0 = C_L > b_S \quad T_s > T$

where T_s denotes the lead time of the synchronization process (set threshold) and T denotes the lead time of the actual measurement data.

From the above-mentioned description, the overall lead time T in the case of batch processes is the time taken to produce a piece of equipment in one period of work. Note that only one person produces one piece of equipment in a batch process, and thus, $T_s = T$. However, in the case of a production flow system, Item no.[1] and Item no.[3] are not appropriate for determining the throughput. In the case of a batch process, only Item no.[2] is not appropriate. The lack of sufficient throughput thus leads to increased costs.

Here, the deviation of the lead time is constrained as follows:

$$\frac{\partial f}{\partial t} = -M_\varphi \frac{\delta f(\varphi)}{\delta \varphi} \tag{59}$$

Equation (59) indicates that the lead time deviation (phase deviation) is an equation to move the surface of lead time function. The cause is dependent on the fluctuation of volatility fluctuation (see Figures 12-14).

As a result, we obtain generally as follows:

$$g(\varphi) = \varphi^2(1-\varphi)^2 \tag{60}$$

$$h(\varphi) = \varphi^2(3-2\varphi) \tag{61}$$

Then,

$$f(\varphi) = \frac{a^2}{2} g(\varphi) + b_S h(\varphi) + c_L\{1 - h(\varphi)\} \tag{62}$$

G-L free energy $F(\varphi)$ is as follows:

$$F(\varphi) = \int_\Omega \left[\frac{\epsilon^2}{2} |\nabla \varphi|^2 + f(\varphi) \right] dV \tag{63}$$

Then,

$$\tau \frac{\partial \varphi}{\partial t} = -\frac{\delta F}{\delta \varphi} \tag{64}$$

By calculation of Equation (64), we obtain as follows:

$$\begin{aligned} \tau \frac{\partial \varphi}{\partial t} &= \epsilon^2 \nabla^2 \varphi + 2a^2 \varphi(1-\varphi) \left\{ \varphi - \frac{1}{2} + \frac{3(c_L - b_S)}{a^2} \right\} \\ &= \epsilon^2 \nabla^2 \varphi + 2a^2 \varphi(1-\varphi) \left\{ \varphi - \frac{1}{2} + \beta \right\}, \quad \beta = \frac{3(c_L - b_S)}{a^2} \end{aligned} \tag{65}$$

The deviation of the throughput average of a monthly period showed a fluctuation of the throughput from September to December, 2014 in Figure 7 and Figure 8. The x-axis of both graphs represents the order date from a customer.

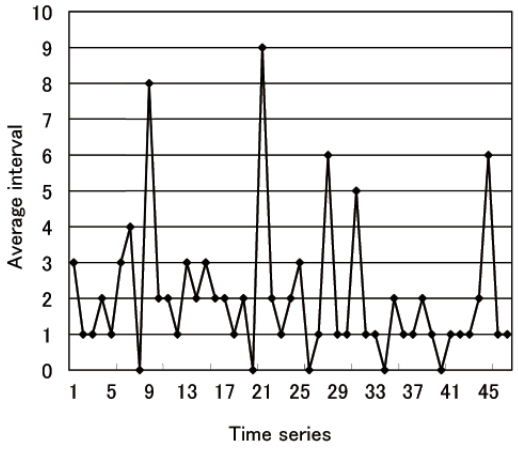

FIGURE 7. Average interval data (September through December, 2014), Average = 2.04, Volatility = 3.7

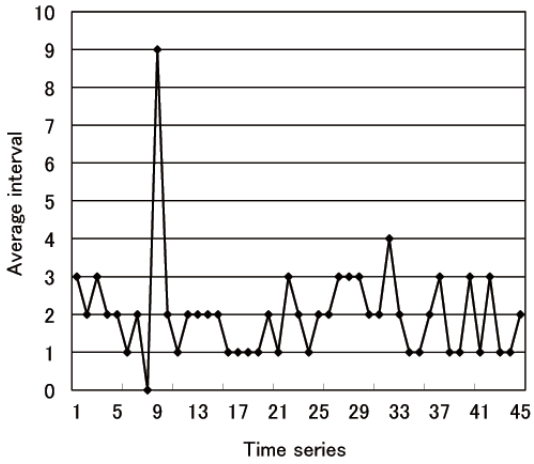

FIGURE 8. Average interval data (September through December, 2014), Average = 2.02, Volatility = 1.8

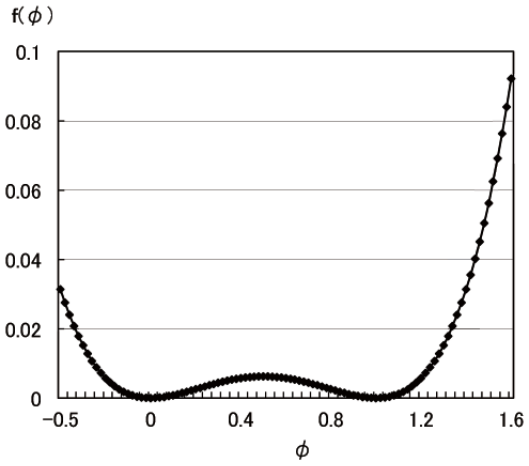

FIGURE 9. Potential function in production processes ($a = 0.1$, $b = 0$, $c = 0$, $0 = b = c$)

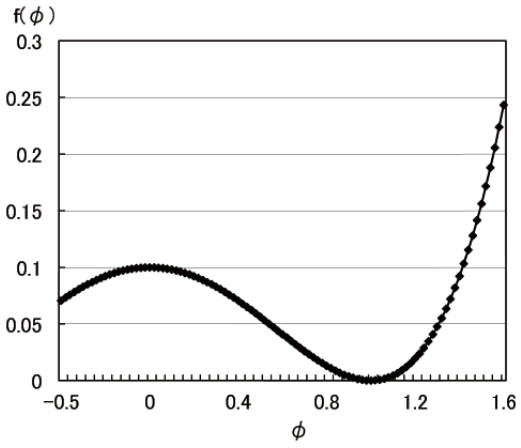

FIGURE 10. Potential function in production processes ($a = 0.1$, $b = 0$, $c = 0.1$, $0 = b < c$)

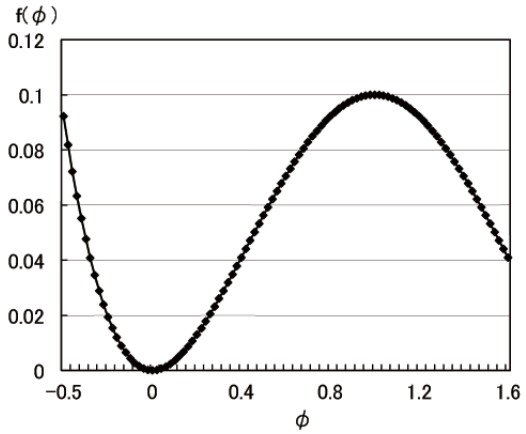

FIGURE 11. Potential function in production processes ($a = 0.1$, $b = 0.1$, $c = 0$, $0 = c < b$)

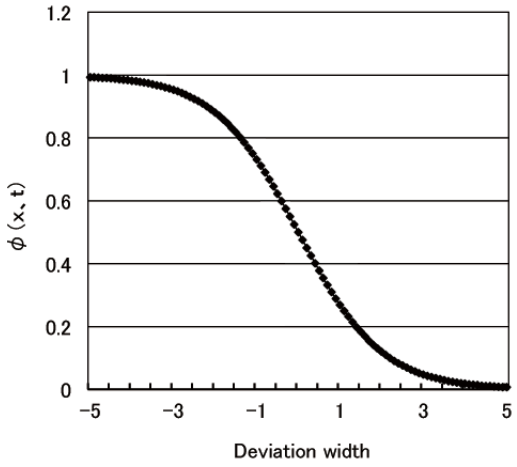

FIGURE 12. Particular solution of normalized lead time ($a = 0.1$, $b = 0$, $c = 0$, $0 = c = b$, $\epsilon = 1$, $V = 0$)

5. **Dynamic Simulation of Production Processes.** We attempted to perform a dynamic simulation of the production process by utilizing the simulation system that NTT DATA Mathematical Systems Inc. (www.msi.co.jp) has developed. With respect to the meaning of the individual parts in Figure 15, we conducted a simulation of the following procedure.

- When the simulation began, it generated one of the products on "generate" parts to "finish".
- In each process, including the six workers in parallel, the slowest worker waited till the work was completed.
- When the work of each process was completed, it moved to the next process.
- Simultaneously as each process was completed, it recorded the working time of each process.

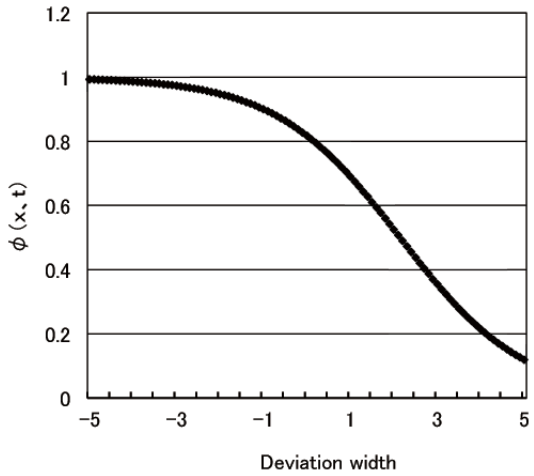

FIGURE 13. Particular solution of normalized lead time ($a = 0.1$, $b = 0.5$, $c = 0$, $0 = c < b$, $\epsilon = 1$, $V = 3$)

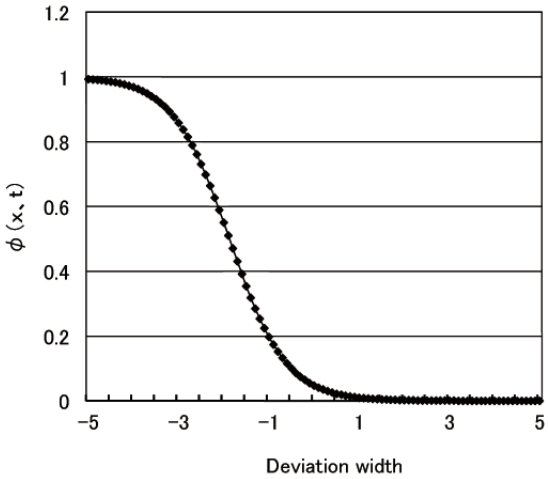

FIGURE 14. Particular solution of normalized lead time ($a = 0.1$, $b = 0$, $c = 1$, $0 = c > b$, $\epsilon = 1$, $V = -6$)

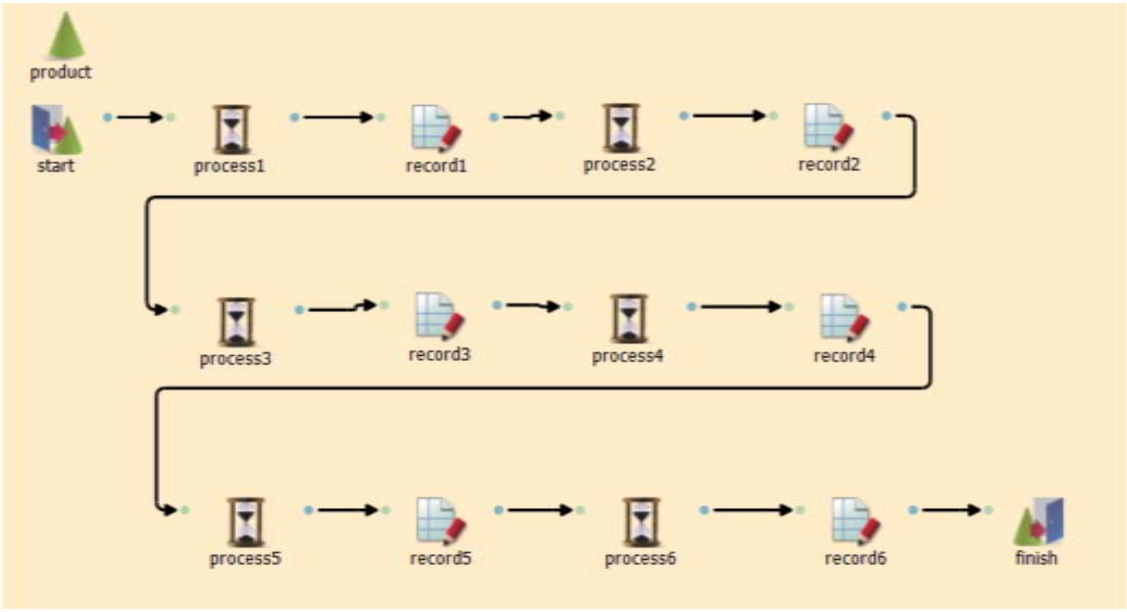

FIGURE 15. Simulation model of production flow system

With respect to Table 2 and Table 3,

- Process No. indicates each process (1-6).
- Average indicates the average time.
- STD indicates the standard deviation of process time (sec).
- Worker efficiency (WE) indicates the efficiency of six workers.

"record" calculates the worker's operating time, which is obtained by multiplying the specified WE data for the log-normally distributed random numbers in Table 2.

Figure 16 shows the operating time of processes 1-6 (record1-record6). As the working time of the synchronous process is less volatile, the work efficiency became higher than the asynchronous process. In Figure 16, the total working time of asynchronous and

TABLE 2. Working data for six production asynchronous processes

Process No.	No.1	No.2	No.3	No.4	No.5	No.6
Average	20	22	25	22	25	21
STD	2.1	2.5	1.6	1.9	2.0	1.9
W.E 1	0.83	1.0	0.66	0.76	0.88	0.91
W.E 2	1.27	1.26	1.21	1.31	1.17	1.20
W.E 3	0.96	1.11	1.01	1.12	0.88	0.89
W.E 4	0.92	0.96	1.06	0.98	0.91	0.9
W.E 5	1.2	1.03	1.07	0.89	1.03	1.1
W.E 6	1.09	1.1	1.2	0.98	1.13	0.89

TABLE 3. Working data for six production synchronous processes

Process No.	No.1	No.2	No.3	No.4	No.5	No.6
Average	20	20	20	20	20	20
STD	1.1	1.5	1.2	1.4	1.0	1.4
W.E 1	1.0	1.0	1.0	1.0	1.0	1.0
W.E 2	1.0	1.0	1.2	1.3	1.1	1.2
W.E 3	1.7	1.1	1.0	1.1	1.0	1.0
W.E 4	1.0	1.0	1.0	1.0	1.0	1.0
W.E 5	1.0	1.0	1.0	1.0	1.0	1.0
W.E 6	1.0	1.3	1.2	1.0	1.1	1.0

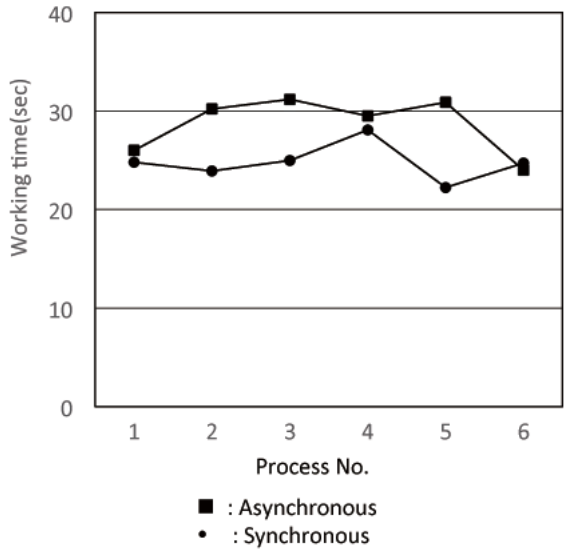

FIGURE 16. Working time for process number one through six

synchronous processes is 1241.7(sec) and 586.4(sec) respectively. The synchronous process shows more better production efficiency than the asynchronous process.

6. **Conclusion.** We discussed the fluctuation of the throughput (lead time) in a production system by applying a phase-field model. We introduced a potential function in the model for describing the throughput volatility as the main parameter.

As a result, Figures 9-11 show that the model can be theoretically applied to understanding real systems. Moreover, we represented Equation (65) for constraining the

throughput deviation. In future work, we will focus on the analysis of fluctuations using Burgers equation for determining the throughput deviation.

REFERENCES

[1] K. Shirai and Y. Amano, Prduction density diffusion equation and production, *IEEJ Trans. Electronics, Information and Systems*, vol.132-C, no.6, pp.983-990, 2012.

[2] K. Shirai and Y. Amano, A study on mathematical analysis of manufacturing lead time – Application for deadline scheduling in manufacturing system, *IEEJ Trans. Electronics, Information and Systems*, vol.132-C, no.12, pp.1973-1981, 2012.

[3] K. Shirai, Y. Amano and S. Omatu, Improving throughput by considering the production process, *International Journal of Innovative Computing, Information and Control*, vol.9, no.12, pp.4917-4930, 2013.

[4] K. Shirai, Y. Amano and S. Omatu, Propagation of working-time delay in production, *International Journal of Innovative Computing, Information and Control*, vol.10, no.1, pp.169-182, 2014.

[5] K. Shirai, Y. Amano and S. Omatu, Process throughput analysis for manufacturing process under incomplete information based on physical approach, *International Journal of Innovative Computing, Information and Control*, vol.9, no.11, pp.4431-4445, 2013.

[6] K. Shirai and Y. Amano, Production throughput evaluation using the Vasicek model, *International Journal of Innovative Computing, Information and Control*, vol.11, no.1, pp.1-17, 2015.

[7] K. Shirai and Y. Amano, On-off intermittency management for production process improvement, *International Journal of Innovative Computing, Information and Control*, vol.11, no.3, pp.815-831, 2015.

[8] K. Shirai and Y. Amano, Throughput improvement strategy for nonlinear characteristics in the production processes, *International Journal of Innovative Computing, Information and Control*, vol.10, no.6, pp.1983-1997, 2014.

[9] K. Shirai and Y. Amano, Evaluation of production process using multimode vibration theory, *International Journal of Innovative Computing, Information and Control*, vol.10, no.3, pp.1161-1178, 2014.

[10] F. Takase, Multi-mode vibration in the group of transmitters coupled lattice, *KURENAI: Kyoto University Research Information Repository*, vol.413, pp.10-29, 1981.

[11] M. Kuramitsu and Y. Nishikawa, A mathematical analysis of self-organization in electrical circuits, *The Society of Instrument and Control Engineers*, vol.29, no.10, pp.899-904, 1990.

[12] M. Kuramitsu and H. Takase, Analysis of multi-degree-of-freedom oscillator with average potential, *IEICE Trans.*, vol.J66-A, no.4, pp.336-343, 1983.

[13] M. Aida and K. Horikawa, Stability analysis for global performance of flow control in high-speed networks based on statistical physics, *IEICE Trans. Commun.*, vol.E82-B, no.12, 1999.

[14] N. G. van Kapmen, A power series expansion of the master equation, *Journal of Physics*, vol.39, pp.551-567, 1961.

[15] R. Kubo, K. Matsuo and K. Kitahara, Fluctuation and relaxation of macrovariables, *Journal of Statistical Physics*, vol.9, pp.51-96, 1973.

[16] K. Shirai and Y. Amano, Self-similarity of fluctuations for throughput deviations within a production process, *International Journal of Innovative Computing, Information and Control*, vol.10, no.3, pp.1001-1016, 2014.

[17] T. Takagi and A. Yamanaka, *Phase Field Method-Material Organization Design by Numerical Simulation*, Yokendo Co., LTD., 2012.

[18] K. Shirai and Y. Amano, Validity of production flow determined by the phase difference in the gradient system of an autonomous decentralized system, *International Journal of Innovative Computing, Information and Control*, vol.10, no.5, pp.1727-1745, 2014.

[19] K. Kitahara, *Statistical Mechanics of Non-equilibrium System*, Iwanami Shoten Co., LTD., 2000.

[20] H. Tasaki, *Thermodynamics – A Contemporary Perspective (New Physics Series)*, Baifukan, Co., LTD., 2000.

Appendix A. **Description of the production stage flow using Riemannian manifolds.** Figure 17 shows the direction of production flow from i through h. Each of the items i, j, and h has a different manifold, and each of the production pathways is also a different manifold.

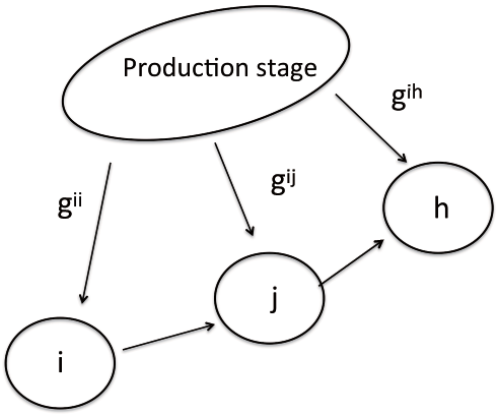

FIGURE 17. Business structure of company of research target

Definition A.1. *The Riemannian manifolds were derived as follows:*

$$E(f) = \int \frac{1}{2}|df|^2 dv_g \tag{66}$$

With a local coordinate system of M to $(x_1, x_2, \cdots, x_m)$ and $(y_1, y_2, \cdots, y_n)$, the corresponding Riemann manifold is as follows:

$$g = \sum_{i,j=1}^{m} g_{ij} dx_i dx_j, \quad h = \sum_{i,j=1}^{n} h_{ij} dx_i dx_j \tag{67}$$

If an inverse matrix is written as (g_{ij}) and (h_{ij}) to (g^{ij}) and (h^{ij}), respectively, then with respect to the matrix $(y_1, y_2, \cdots, y_n)$, a Christoffel symbol to ${}^N\Gamma_{ij}^k$ is written as follows:

$${}^N\Gamma_{ij}^k = \frac{1}{2} \sum_{l=1}^{n} h^{kl} \left\{ \frac{\partial h_{jl}}{\partial y_i} + \frac{\partial h_{il}}{\partial y_j} - \frac{\partial h_{ij}}{\partial y_l} \right\} \tag{68}$$

In the same manner of Equation (68), we establish ${}^M\Gamma_{ij}^k$ with respect to $(x_1, x_2, \cdots, x_m)$ of g.

We establish Laplace operator's Δ_g of (M, g) as follows:

$$\Delta_g = \sum_{i,j=1}^{m} g^{ij} \left\{ \frac{\partial^2}{\partial x_i \partial x_j} - \sum_{k=1}^{m} {}^M\Gamma_{ij}^k \frac{\partial}{\partial x_k} \right\} \tag{69}$$

Here, the mapping f using a local coordinate system,

$$f = (f_1, f_2, \cdots, f_n), \ f_i = y_i \circ f \tag{70}$$

$$f_i = f_i(f_1, f_2, \cdots, f_n) \tag{71}$$

From Equations (70) and (71), the equation of harmonic maps is as follows:

$$\Delta_g f^k = \sum_{i,j,k,l=1}^{m} g^{klN} \Gamma_{ij}^k(f) \frac{\partial f^i}{\partial x_k} \frac{\partial f^j}{\partial x_l} = 0, \quad k = 1, 2, \cdots, n \tag{72}$$

Equation (72) is a quasi-linear second-order elliptic type.

$$Af = -div(grad_G f) + \sum_i b^i \partial_i f \tag{73}$$

where b^i is elements of the flow velocity vector, which indicates $\mathbf{b} = (\mathbf{b^1}, \mathbf{b^2}, \cdots, \mathbf{b^n})$.

Appendix B. **Diffusion equation for production processes.** If an external force (control force) does not work, then each process element will converge to a uniform solution and thus the finished product will not have a set deadline. In other words, this will indicate a product with a natural timeline of production.

$$\frac{\partial S(x,t)}{\partial t} = \mathcal{L}S = div(grad_G S) \tag{74}$$

The left term of Equation (74) saves the total load $\sum_{(x,t)\in\Omega\times D} S(x,t)$, and thus the corresponding load balancing solution is as follows:

$$\bar{S} = \frac{\sum S(x,t)}{[\Omega \times D]} \tag{75}$$

Monotonically decrease the square error $\sum S(x,t) - \bar{S}$.

The saving of total load is as follows:

$$\int_M div(grad_G S(x,t))dx = -\int_M \mathcal{L}S(x,t)dx = 0 \tag{76}$$

$$\sum \frac{\partial S(x,t)}{\partial t} = -\sum \mathcal{L}S(x,t) = 0 \tag{77}$$

$\mathcal{L}S(x,t)$ has different metrics (Average and Volatility), which also refer to the Riemannian metrics on each process and transport function.

$$\mathcal{L}S(x,t) = \sum_{i,j} g^{ij}(x) \left\{ \frac{\partial^2 S(x,t)}{\partial x^i \partial x^j} - \sum_{ik} \partial_i g^{ik}(x) \right\} \tag{78}$$

$$div(X) = \sum_i \partial_i X^i, \;\; grad_G f = \sum_{ij} g^{ij} \partial_j f \partial_i \tag{79}$$

$$\begin{aligned} \frac{\partial S(u,t)}{\partial t} &= \mathcal{L}S(u,t) \\ &= -\sum_{ij} g^{ij}(x) \left[\frac{\partial^2 S(u,t)}{\partial x^i \partial x^j} - \sum_{ij} \partial_i g^{ik}(x) \frac{\partial S(u,t)}{\partial u} \right] \end{aligned} \tag{80}$$